SCIENCE CHINA
Information Sciences

• RESEARCH PAPER •

December 2019, Vol. 62 222203:1–222203:13
https://doi.org/10.1007/s11432-018-9864-8

Dynamical model of HEV with two planetary gear units and its application to optimization of energy consumption

Jiangyan ZHANG[1*], Shota INUZUKA[2], Takafumi KOJIMA[2], Tielong SHEN[2] & Junichi KAKO[3]

[1]*College of Mechanical and Electronic Engineering, Dalian Minzu University, Dalian* 116600*, China;*
[2]*Department of Engineering and Applied Sciences, Sophia University, Tokyo* 102-8554*, Japan;*
[3]*Higashi-Fuji Research Center, Toyota Motor Corporation, Shizuoka* 410-1107*, Japan*

Received 10 December 2018/Accepted 4 March 2019/Published online 12 November 2019

Abstract A hybrid electric vehicle (HEV) that uses multiple planetary gear units with clutches as transmission system is advanced for the powertrain performance, because the operation of the clutches can lead to distinct operating modes, and the induced possible operating modes provide additional freedom to deal with the energy optimal control problem. Under each operating mode, the powertrain mechanical system has specific dynamical behavior. In order to develop model-based optimization schemes that can tackle the transient operations of the vehicle, exact dynamical modeling is investigated focusing on a hybrid powertrain system that uses a two-planetary-gear transmission box with two clutches. It shows that according to the states of the two clutches, the powertrain system has the power-split mode, parallel mode and the electric vehicle (EV) mode. Finally, an analysis for the calculation of the desired driving torque and its application to the dynamic programming (DP)-based energy management indicate the significance of the developed exact dynamical models.

Keywords hybrid electric vehicle, two-planetary-gear, modeling, energy management, dynamic programming

Citation Zhang J Y, Inuzuka S, Kojima T, et al. Dynamical model of HEV with two planetary gear units and its application to optimization of energy consumption. Sci China Inf Sci, 2019, 62(12): 222203, https://doi.org/10.1007/s11432-018-9864-8

1 Introduction

The efficiency of hybrid electric vehicles (HEVs) has been improved through the intelligent management of the electric battery and fuel energy use. HEV powertrains are generally divided into two categories, parallel and series, depending on the transmission system that connects the electric devices and the combustion engine [1]. Planetary gear (PG) units enable various operating modes (parallel, series and power-split modes) by switching and/or controlling the clutches and energy devices, thus enhancing the energy efficiency of the powertrain [2, 3]. Meanwhile, the energy management problem of HEVs has been tackled by diverse approaches, such as dynamic programming (DP)-based strategies [4–8], model predictive control (MPC)-based design methods [9–11], stochastic MPC-based approaches [12, 13], and logical dynamic system theory-based approaches [14]. Indeed, energy management has been a focal research topic for over two decades, and is usually investigated in dynamical models of the battery and the powertrain.

* Corresponding author (email: zhangjy@sophia.ac.jp)

The energy management of HEVs with PG units has been solved using a DP algorithm, providing a benchmark optimal solution [4–7]. Meanwhile, MPC-based methods [9, 10] have provided optimal solutions in real-time applications. In most contributions [4–10], the demand power distribution has been realized through model-based control design. The demand power is usually determined from the vehicle speed in a one-dimensional dynamical model. In the vehicle powertrain dynamical model, the demand power must be sufficient to drive all the rotational devices as well as the vehicle itself. The one-dimensional model of vehicle powertrain dynamics assumes that all the rotational gears are connected. However, in the HEV powertrains that use multi PG units and clutches, the involved rotating gears depend on the states of the clutches [2, 15]. By switching the clutch states, one can change the mechanical dynamics of the powertrain system. The present paper demonstrates that the mechanical dynamics of the PG unit are not one-dimensional; rather, changing the clutch states, i.e., operating mode, alters the equivalent inertia of the rotational dynamics. Therefore, the one-dimensional dynamic model will limit the accuracy of the demand power calculation. Accurate powertrain modeling is essential for developing and evaluating model-based HEV control schemes.

The present paper develops an exact dynamical model that simulates the mechanical dynamics of a HEV powertrain with two PG units and two clutches. The study shows that the rotational dynamics in power-split mode are coordinated by the rotational speed of any two axes in the gear box. Using the developed models with the parameters of a prototype vehicle, it then demonstrates a dynamic planning-based energy management strategy. The control inputs are the torque commands of the engine, generator and motor, and the operations of both clutches. The optimization problem is dynamically constrained by the two dimensional dynamics powered by the battery. In this strategy, the demand torque depends not only on the vehicle speed but also on the reference speed of the engine.

2 Preliminary

The PG unit is a well-known power-split device that has been successfully employed in HEVs [1]. A typical PG unit comprises sun, ring, and carrier gears connected to different power sources. The output power of the PG unit must satisfy the driver demand power, which usually propels the vehicle. Under this constraint, one can assign the rotational speed of each gear and torques provided by the power sources that minimize the energy consumption. Figure 1 shows the architecture of the HEV powertrain considered in this paper. The powertrain comprises two PG units with two clutches. A combustion engine and generator are connected to the sun and carrier gears of unit I, respectively, and a motor is connected to the sun gear of unit II. The two ring gears of the PG units are connected by clutch 2 (CL2), and the generator is connected to the body of the powertrain by clutch 1 (CL1). The ring gear of unit II, which outputs the propulsion torque, is connected to the differential gear, while the carrier gear of unit II is fixed. In Figure 1, τ_{e}, τ_{m} and τ_{g} denote the engine, motor, and generator torques, respectively, ω_{e}, ω_{m} and ω_{g} denote the speeds of the engine, motor, and generator, respectively, and v is the longitudinal speed of the vehicle.

As is evident from its mechanical topology, the powertrain can be configured to EV, parallel, or power-split mode by changing the clutch operation. These three operation modes are described below.

(a) EV mode. When CL2 is released (power off), the output torque from the motor is passed only through the sun gear. In this case, both the engine and generator are detached from the driveline.

(b) Parallel mode. When both clutches are engaged (power on), the generator is detached from the powertrain because the sun gear of unit I is fixed by CL1. The engine provides the driving power that passes through the ring gear of unit II to the other ring gear, and combines with the motor power to propel the vehicle.

(c) Power-split mode. When CL1 is on while CL2 is off, the two PG units are combined into a single unit. In this mode, the generator both starts the engine and regulates its speed at the desired value. The powertrain is a power-split structure that efficiently optimizes the consumption of the energy generated by the fuel and electricity with two degrees of freedom, thus managing the power sources.

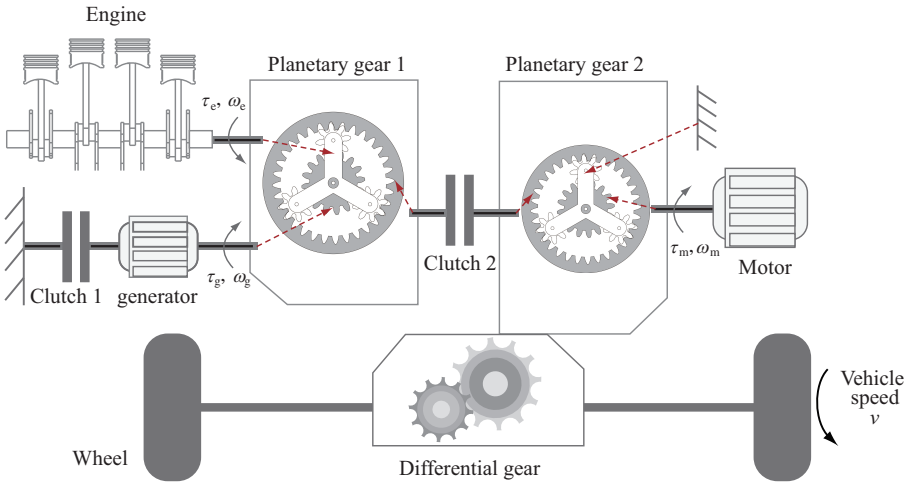

Figure 1 (Color online) Configuration of the HEV powertrain with two planetary gears.

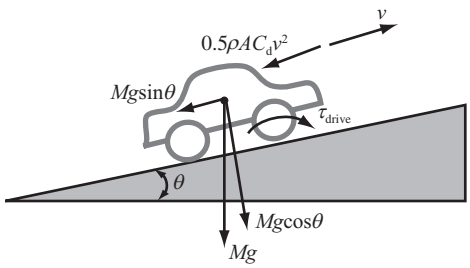

Figure 2 Illustration of vehicle moving and forces.

It should be noted that in the power-split mode, the rotational speed of each gear is not uniformly decided by the geometrical structure of the gears. Instead, it follows the energy conservation law. In the next section, we demonstrate that the mechanical dynamics of the PG unit in this mode is a two-dimensional dynamical system. Therefore, the kinetic energy of the gear unit (particularly in transient mode) should be calculated through a two-dimensional coupled mass system.

To simplify the torque calculation, most of the literature reports on energy management strategies treat the powertrain as a one-dimensional mass system (see Figure 2). In this case, the required torque is a simple function of the vehicle speed v. Then, the vehicle dynamics are simply described as follows:

$$M\dot{v} = \frac{\tau_{\text{drive}} - \tau_{\text{B}}}{R_{\text{tire}}} - F(v), \tag{1}$$

where M, τ_{drive}, τ_{B} and R_{tire} denote the vehicle mass, driving torque, friction braking torque and wheel radius of the tire, respectively, and $F(v)$ is the road load represented by

$$F(v) = Mg(\mu_{\text{r}}\cos\theta + \sin\theta) + \frac{1}{2}\rho AC_{\text{d}}v^2, \tag{2}$$

where g, μ_{r} and θ denote the gravitational acceleration, coefficient of rolling resistance and road slope, respectively, and ρ, A and C_{d} denote the air density, frontal area of the vehicle and drag coefficient, respectively. Based on the aforementioned dynamical equation, the demand torque τ^*_{drive} that propels the vehicle at the desired speed v_{d} and acceleration $\dot{v}_{\text{d}}$ is given as follows:

$$\tau^*_{\text{drive}} = M\dot{v}_{\text{d}}R_{\text{tire}} + F(v_{\text{d}}).$$

As clarified in the powertrain system configuration, the equivalent vehicle mass M must involve the rotational motion energy of the gears. This means that in different modes, the equivalent mass M must be reset to match the kinetic energy of the different operating gears. Particularly in the power-split mode,

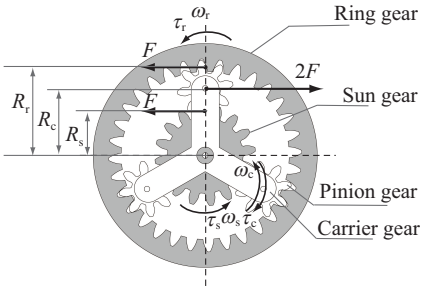

Figure 3 Mechanics of a planetary gear unit.

the acceleration energy of PG unit II contributes to the demand power. In the next section, the exact models of the powertrain system will be deduced to characterize the dynamics of each operating mode and to indict the significance at the transient process when the operating mode changes.

3 Modeling

The main device of the considered HEV powertrain is the PG unit. The mechanical configuration of a PG unit is shown in Figure 3. The radii of the sun, carrier, and ring gears, denoted as $R_{\rm s}$, $R_{\rm c}$ and $R_{\rm r}$, respectively, are related as follows:

$$R_{\rm s} + R_{\rm r} = 2R_{\rm c}. \tag{3}$$

When the gears move, the carrier gear transfers kinetic energy to the ring and sun gears through several pinion gears. The internal forces F, F, and $2F$ act at the ring gear, sun gear and carrier gear are shown in Figure 3. Let $\omega_{\rm r}$, $\omega_{\rm s}$ and $\omega_{\rm c}$ denote the speeds of the ring, sun, and carrier gears, respectively, and let the corresponding torques be $\tau_{\rm r}$, $\tau_{\rm s}$ and $\tau_{\rm c}$, respectively. Noting that $\tau_{\rm r} = FR_{\rm r}$, $\tau_{\rm s} = FR_{\rm s}$ and $\tau_{\rm c} = 2FR_{\rm c}$, the power conservation law dictates that

$$FR_{\rm r}\omega_{\rm r} + FR_{\rm s}\omega_{\rm s} = 2FR_{\rm c}\omega_{\rm c}. \tag{4}$$

Combining relations (3) and (4) gives the following mechanical property:

$$R_{\rm r}\omega_{\rm r} + R_{\rm s}\omega_{\rm s} = 2(R_{\rm r} + R_{\rm s})\omega_{\rm c}. \tag{5}$$

Based on mechanical physics principles (5), the dynamical models of the powertrain system shown in Figure 1 are deduced as follows. By Newton's second law, the mechanical dynamics of the powertrain system are characterized by the speed of each rotational device. Before presenting the dynamics, we suppose that all connections in the two PG units are rigid and that the friction loss is negligible. In this case, the rotational speeds of the motor, engine, and generator are related as follows:

$$\omega_{\rm m} = \omega_{\rm s2}, \tag{6}$$

$$\omega_{\rm e} = \omega_{\rm c1}, \tag{7}$$

$$\omega_{\rm g} = \omega_{\rm s1}, \quad \text{if clutch 1 is "off"}, \tag{8}$$

where $\omega_{\rm s1}$ and $\omega_{\rm s2}$ denote the speeds of the sun gears of PG1 and PG2, respectively, and $\omega_{\rm c1}$ denotes the speed of the carrier gear of PG1. With the above speed relations, we derive the dynamical models of the powertrain system in each operating mode.

First, we obtain the speed relations among the rotators of the powertrain mechanical system in power-split mode. In this mode, the ring gears of PG1 and PG2 are combined by the CL2 and rotate at the same speed, i.e.,

$$\omega_{\rm r1} = \omega_{\rm r2} := \omega_{\rm r}, \tag{9}$$

where ω_{r1} and ω_{r2} denote the speeds of the PG1 and PG2 ring gears, respectively. The engine and generator deliver torques through PG1 to PG2. From (5), (7)–(9), the speeds of the engine, generator, and ring gear are related as follows:

$$R_{r1}\omega_r + R_{s1}\omega_g = (R_{r1} + R_{s1})\omega_e, \tag{10}$$

where R_{r1} and R_{s1} denote the radii of the ring and sun gears of PG1, respectively. As shown in Figure 1, the PG2 system transfers the driving torques from the engine, generator, and motor to the vehicle propeller shaft through the differential gear. As the carrier gear of PG2 is locked, the motor torque is delivered by the sun gear to the ring gear directly through the pinion gears, so the motor speed and ring-gear speed are related as follows:

$$\omega_r R_{r2} = \omega_m R_{s2}, \tag{11}$$

where R_{s2} and R_{r2} denote the radii of the sun and ring gears of PG2, respectively. Let g_r denote the gear ratio of the differential gear. The output speed of the differential gear ω_t then relates to the ring-gear speed as follows:

$$\omega_t = \frac{1}{g_r}\omega_r. \tag{12}$$

The rotational speed of the vehicle wheel ω_w is the following function of the differential gear speed:

$$\omega_w = \frac{1}{g_f}\omega_t, \tag{13}$$

where g_f denotes the final differential ratio. As $v = \omega_w R_{tire}$, Eqs. (12) and (13) imply the following relationships between the ring gear and vehicle speeds:

$$\omega_r = G_{rf} v, \quad \text{with} \quad G_{rf} = g_r g_f \frac{1}{R_{tire}}. \tag{14}$$

Combined with Eq. (11), this expression gives

$$\omega_m = \epsilon_2 G_{rf} v, \tag{15}$$

where $\epsilon_2 = R_{r2}/R_{s2}$. Finally, substituting (14) into (5), we obtain the following:

$$\omega_g = (1 + \epsilon_1)\omega_e - \epsilon_1 G_{rf} v, \tag{16}$$

where $\epsilon_1 = R_{r1}/R_{s1}$. This implies that at vehicle speed v, the engine speed can be regulated by the generator.

Before presenting the dynamical models of the powertrain system in power-split mode, we describe the dynamics of the individual components (the power input sources, transfer gears, and shafts). Let F_1 denote the internal force acting on the ring and sun gears of PG1, and let τ_{cl} denote the torque on CL2. Considering the mechanical physics of the PG units, the dynamical operation of the PG1 system is governed by the following equations:

$$I_e\dot{\omega}_e = \tau_e - R_{r1}F_1 - R_{s1}F_1, \tag{17a}$$

$$I_g\dot{\omega}_g = \tau_g + R_{s1}F_1, \tag{17b}$$

$$I_{r1}\dot{\omega}_r = R_{r1}F_1 - \tau_{cl}, \tag{17c}$$

where I_e and I_g denote the combined inertias of the engine and generator with their connected corresponding gears, respectively, and I_{r1} denotes the inertia of the ring gear of PG1. The internal force F_2 acts on the ring and sun gears of PG2. The speed dynamics associated with the PG2 gears are then expressed as follows:

$$I_m\dot{\omega}_m = \tau_m - R_{s2}F_2, \tag{18a}$$

$$I_{\mathrm{r}2}\dot{\omega}_{\mathrm{r}} = \tau_{\mathrm{cl}} + R_{\mathrm{r}2}F_2 - \tau_{\mathrm{rt}}, \tag{18b}$$

where I_{m} denotes the combined inertias of the motor and its connected sun gear, $I_{\mathrm{r}2}$ denotes the inertia of the ring gear of PG2, and τ_{rt} denotes the torque on the driving gear of the differential gear. Finally, the speed dynamics of the driven gear of the differential gear can be expressed as follows:

$$I_t\dot{\omega}_t = g_{\mathrm{r}}\tau_{\mathrm{rt}} - \tau_{\mathrm{pera}}, \tag{19}$$

where I_t denotes the inertia of the differential gear, and τ_{pera} denotes the torque acting on the propeller shaft.

Now consider that friction loss occurs from the propeller shaft torque τ_{pera} to the driving torque τ_{drive}. As an analytical expression for the efficiency is unavailable, we apply the following statistical fitting:

$$\tau_{\mathrm{drive}} = g_{\mathrm{f}}(A_\eta(v) + B_\eta\tau_{\mathrm{pera}}), \tag{20}$$

where $A_\eta(v)$ and B_η are obtained through model identification. From the aforementioned speed relations (14)–(16), we note that the system dynamics (17)–(19) can be combined by eliminating the immeasurable variables. First, we eliminate F_2, τ_{rt} and τ_{pera} by rearranging the dynamical equations (18) and (19) as follows:

$$M_\Sigma\dot{v} = \mathcal{A}\tau_{\mathrm{m}} + \mathcal{B}\tau_{\mathrm{cl}} - \tilde{F}(v) - \frac{\tau_{\mathrm{B}}}{R_{\mathrm{tire}}} \tag{21}$$

with

$$M_\Sigma = [g_{\mathrm{r}}^2(I_{\mathrm{m}}\epsilon_2^2 + I_{\mathrm{r}2}) + I_t]\frac{g_{\mathrm{f}}^2 B_\eta}{R_{\mathrm{tire}}^2} + M, \quad \mathcal{A} = \epsilon_2 G_{\mathrm{rf}} B_\eta, \quad \mathcal{B} = G_{\mathrm{rf}} B_\eta,$$

and

$$\tilde{F}(v) = F(v) - \frac{A_\eta(v) g_{\mathrm{f}}}{R_{\mathrm{tire}}}.$$

Considering (16) and eliminating the F_1 from the dynamics (17a) and (17b), we obtain

$$a_{11}\dot{\omega}_{\mathrm{e}} + a_{12}\dot{v} = \tau_{\mathrm{e}} + b_{11}\tau_{\mathrm{g}}. \tag{22}$$

Considering (14), eliminating F_1 and τ_{cl} from the dynamic equations (17a) and (17c), and combining with (21), we then obtain the following:

$$a_{21}\dot{\omega}_{\mathrm{e}} + a_{22}\dot{v} = b_{21}\tau_{\mathrm{m}} + b_{22}\tau_{\mathrm{e}} - \tilde{F}(v) - \frac{\tau_{\mathrm{B}}}{R_{\mathrm{tire}}}, \tag{23}$$

where

$$a_{11} = I_{\mathrm{e}} + I_{\mathrm{g}}(1+\epsilon_1^2), \quad a_{12} = -I_{\mathrm{g}}(1+\epsilon_1)\epsilon_1 G_{\mathrm{rf}}, \quad b_{11} = 1+\epsilon_1,$$
$$a_{21} = \frac{\mathcal{B}}{1+\epsilon_1} I_{\mathrm{e}}, \quad a_{22} = M_\Sigma + \mathcal{B}G_{\mathrm{rf}}I_{\mathrm{r}1}, \quad b_{21} = \mathcal{A}, \quad b_{22} = \frac{\mathcal{B}}{1+\epsilon_1}.$$

The above-derived Eqs. (22) and (23) characterize the mechanical dynamics of the powertrain system by a two-dimensional differential equation in terms of the engine and vehicle speeds alone.

In parallel mode, the generator with the connected sun gear of PG1 is locked by CL1, so $R_{\mathrm{s}1}F_1 = 0$ and $\omega_{\mathrm{g}} = 0$. In this mode, the PG1 system is a one-degree-of-freedom transmission gear through which the engine supplies a driving torque to the propeller shaft in parallel with the motor. The speed constraint of PG1 (10) then alters to the following:

$$\omega_{\mathrm{e}} = \frac{\epsilon_1}{1+\epsilon_1} G_{\mathrm{rf}} v, \tag{24}$$

and the engine dynamics (17a) reduce to the following:

$$I_{\mathrm{e}}\dot{\omega}_{\mathrm{e}} = I_{\mathrm{e}} - R_{\mathrm{r}1}F_1. \tag{25}$$

Owing to the PG1 mechanics in this mode, the mechanical dynamics of the powertrain system have only one free variable. Merging the dynamic equations (25), (17c) and (21) to eliminate F_1 and $\tau_{\rm cl}$, we obtain the following dynamical equation:

$$\left[M_\Sigma + \mathcal{B}G_{\rm rf}\left(\frac{\epsilon_1}{1+\epsilon_1}I_{\rm e} + I_{\rm r1}\right)\right]\dot{v} = \mathcal{A}\tau_{\rm m} + \mathcal{B}\tau_{\rm e} - \tilde{F}(v) - \frac{\tau_{\rm B}}{R_{\rm tire}}. \tag{26}$$

In EV mode, the PG2 system is cut off from the transmission system; therefore, the mechanical dynamics are governed by (21) with $\tau_{\rm cl} = 0$. Further, the motor speed is calculated by (15).

Finally, let $u_{\rm c1}$ and $u_{\rm c2}$ denote the states of the clutches CL1 and CL2, respectively. The clutch state u_{ci} is a binary variable equaling 0 if clutch i is off and 1 if clutch i is on. Then, the mechanical dynamics of the powertrain system in the three operating modes are summarized as follows:

- When $(u_{\rm c1}, u_{\rm c2}) = (0, 0)$, the powertrain model is

$$M_\Sigma\dot{v} = \mathcal{A}\tau_{\rm m} - \tilde{F}(v) - \frac{\tau_{\rm B}}{R_{\rm tire}}, \tag{27a}$$

$$\begin{cases} \omega_{\rm m} = \epsilon_2 G_{\rm rf} v, \\ \omega_{\rm e} = 0, \\ \omega_{\rm g} = 0. \end{cases} \tag{27b}$$

- When $(u_{\rm c1}, u_{\rm c2}) = (1, 1)$, the powertrain model is

$$(M_\Sigma + M_E)\dot{v} = \mathcal{A}\tau_{\rm m} - \tilde{F}(v) - \frac{\tau_{\rm B}}{R_{\rm tire}}, \tag{28a}$$

$$\begin{cases} \omega_{\rm m} = \epsilon_2 G_{\rm rf} v, \\ \omega_{\rm e} = \dfrac{\epsilon_1}{1+\epsilon_1} G_{\rm rf} v, \\ \omega_{\rm g} = 0, \end{cases} \tag{28b}$$

$$\text{with } M_E = \mathcal{B}G_{\rm rf}\left(\frac{\epsilon_1}{1+\epsilon_1}I_{\rm e} + I_{\rm r1}\right).$$

- When $(u_{\rm c1}, u_{\rm c2}) = (0, 1)$, the powertrain model is

$$\begin{bmatrix} \dot{\omega}_{\rm e} \\ \dot{v} \end{bmatrix} = \begin{bmatrix} a_{11} & a_{12} \\ a_{21} & a_{22} \end{bmatrix}^{-1} \begin{bmatrix} \tau_{\rm e} + b_{11}\tau_{\rm g} \\ b_{21}\tau_{\rm m} + b_{22}\tau_{\rm e} - \tilde{F}(v) - \dfrac{\tau_{\rm B}}{R_{\rm tire}} \end{bmatrix}, \tag{29a}$$

$$\begin{cases} \omega_{\rm m} = \epsilon_2 G_{\rm rf} v, \\ \omega_{\rm g} = (1+\epsilon_1)\omega_{\rm e} - \epsilon_1 G_{\rm rf} v. \end{cases} \tag{29b}$$

4 Application to energy management

The deduced dynamical models (27a), (28a), and (29a) accurately describe the mechanical dynamics in different operating modes. According to these models, the moments of inertia (in terms of the vehicle speed dynamics) significantly differ between the parallel and EV modes, whereas in power-split mode, the vehicle speed dynamics are coupled with the engine speed dynamics. To guarantee the desired operating speed of the vehicle, the demand driving torque supplied by the motor and/or the engine/generator unit depends on the operating modes. In particular, the demand driving torque in power-split mode should manage the transient operations of the engine. As a demonstration, this section accurately calculates the demand driving torque using the deduced models. After determining the exact driving-torque demand for a given driving route, a DP strategy that accounts for the transient engine operation is proposed for optimizing the energy-distribution control problem.

Table 1 Main parameters of the HEV model

Parameter	Value	Unit
Vehicle mass M	1733.5	kg
Wheel radius R_{tire}	0.305	m
Front area A	2.16	m^2
Engine inertia I_{e}	0.141	$\text{km}\cdot\text{m}^2$
Motor inertia I_{m}	0.0154	$\text{km}\cdot\text{m}^2$
Generator inertia I_{g}	0.074	$\text{km}\cdot\text{m}^2$
Ring gear inertia of PG1 I_{r1}	10^{-10}	$\text{km}\cdot\text{m}^2$
Ring gear inertia of PG1 I_{r2}	10^{-10}	$\text{km}\cdot\text{m}^2$
Differential gear inertia I_{t}	10^{-10}	$\text{km}\cdot\text{m}^2$
PG1 gear ratio ϵ_1	2.6	–
PG1 gear ratio ϵ_2	3.8	–
Differential gear ratio g_{r}	0.43	–
Final differential ratio g_{f}	3.95	–

4.1 Desired driving torque calculation

Let v_{d} be the desired vehicle speed. Herein, we derive the demand driving torque that must be supplied by the motor and/or engine/generator unit to guarantee the vehicle driving along v_{d}. Note that the demand driving torque actually includes two components: one for generating the desired vehicle acceleration, the other for overcoming the road load. The demand driving torque in the three operating modes can be calculated from the corresponding dynamical models (27a), (28a), and (29a), as described below:

• Based on the dynamical model (27a), the demand driving torque $\tau^{\text{I}}_{\text{drive}}$ in EV mode is calculated as follows:

$$T^{\text{I}}_{\text{drive}} = M_{\Sigma}\dot{v}_{\text{d}} + \tilde{F}(v_{\text{d}}). \tag{30}$$

• Based on the dynamical model (28a), the demand driving torque $\tau^{\text{II}}_{\text{drive}}$ in parallel mode is given as follows:

$$T^{\text{II}}_{\text{drive}} = \left[M_{\Sigma} + \mathcal{B}G_{\text{rf}}\left(\frac{\epsilon_1}{1+\epsilon_1}I_{\text{e}} + I_{\text{r1}}\right)\right]\dot{v}_{\text{d}} + \tilde{F}(v_{\text{d}}). \tag{31}$$

• In the system dynamics (29a) of power-split mode, the driving-demand torque should regulate both the desired vehicle speed and the desired engine speed ω_{ed}; hence, the driving torque demand comprises two components, $T^{\text{III}}_{\text{drive1}}$ and $T^{\text{III}}_{\text{drive2}}$, which can be calculated as follows:

$$\begin{bmatrix} T^{\text{III}}_{\text{drive1}} \\ T^{\text{III}}_{\text{drive2}} \end{bmatrix} = \begin{bmatrix} a_{11} & a_{12} \\ a_{21} & a_{22} \end{bmatrix} \begin{bmatrix} \dot{\omega}_{\text{ed}} \\ \dot{v}_{\text{d}} \end{bmatrix} + \begin{bmatrix} 0 \\ \tilde{F}(v_{\text{d}}) \end{bmatrix}. \tag{32}$$

Clearly, the demand driving torque in power-split mode depends not only on the acceleration of the vehicle but also on the engine speed variation. The demand torque apportioned to the engine trajectory is considerable, particularly during transient operations.

Finally, it should be noted that the derived control-oriented dynamical HEV model supposes a rigid connected gear and negligible friction loss; hence, the energy expended by the gear operation during driving was omitted from the control design.

4.2 Optimal energy management

In this subsection, the considered HEV powertrain is globally optimized by the DP algorithm. The main parameters of the powertrain system model are shown in Table 1. The design objective of the DP strategy is to find a control policy $u(k)$ $(k = 0, \ldots, N-1)$ that minimizes the equivalent energy consumption in driving cycle $v_{\text{d}}(k)$. The cost function to be minimized is given as follows:

$$J = \sum_{k=0}^{N-1} (m_{\text{f}}(k) + \Gamma_{\text{e}} m_{\text{e}}(k))\Delta t, \tag{33}$$

where m_{f} (g/s) denotes the fuel flow rate, m_{e} (w) denotes the instantaneous electricity consumption, and Γ_{e} is the fuel-electricity equivalent weighting factor. In the control design, the analytical expressions for the fuel flow rate are derived from the map data of the engine, and the instantaneous electricity consumption is derived from the map data of the motor and generator. By matching the fuel flow rate to the map data, i.e., $m_{\mathrm{f}} = M_{\mathrm{f}}(\omega_{\mathrm{e}}, \tau_{\mathrm{e}})$, a polynomial expression was derived for the fuel flow rate with respect to the engine operating point $(\omega_{\mathrm{e}}, \tau_{\mathrm{e}})$. The instantaneous electricity consumption was obtained from the battery model in the HEV. The battery is usually modeled as an open-circuit voltage system in which the battery power flow is given as follows:

$$P_{\mathrm{b}} = U_{\mathrm{o}} I_{\mathrm{b}} - I_{\mathrm{b}}^2 R_{\mathrm{b}}, \tag{34}$$

where U_{o}, I_{b} and R_{b} denote the open circuit voltage, the current and the internal resistance of the battery, respectively. The battery power flow P_{b} depends on the powers of the motor and generator as follows:

$$P_{\mathrm{b}} = \tau_{\mathrm{m}}\omega_{\mathrm{m}} + \tau_{\mathrm{g}}\omega_{\mathrm{g}} + P_{\mathrm{m}}^{\mathrm{loss}}(\tau_{\mathrm{m}}, \omega_{\mathrm{m}}) + P_{\mathrm{g}}^{\mathrm{loss}}(\tau_{\mathrm{g}}, \omega_{\mathrm{g}}), \tag{35}$$

where $P_{\mathrm{m}}^{\mathrm{loss}}$ and $P_{\mathrm{g}}^{\mathrm{loss}}$ denote the operating point-dependent power losses of the motor and generator, respectively. The instantaneous electricity consumption is characterized by the battery state of charge (SoC), given by

$$m_{\mathrm{e}} = -U_{\mathrm{o}} Q_{\mathrm{b}} \dot{\mathrm{SoC}}, \tag{36}$$

where Q_{b} denotes the maximum charge capacity of the battery. The variation in the battery SoC is calculated as follows:

$$\dot{\mathrm{SoC}} = \frac{-U_{\mathrm{o}} + \sqrt{U_{\mathrm{o}}^2 - 4R_{\mathrm{b}}P_{\mathrm{b}}(\tau_{\mathrm{m}}, \omega_{\mathrm{m}}, \tau_{\mathrm{g}}\omega_{\mathrm{g}})}}{2Q_{\mathrm{b}}R_{\mathrm{b}}}. \tag{37}$$

In the control design, the power losses of the motor and generator were analytically derived from the corresponding map data.

The control variables of the energy management problem are $u = [u_{\mathrm{c}1}, u_{\mathrm{c}2}, \tau_{\mathrm{e}}, \omega_{\mathrm{e}}]$. Along a given driving route v_{d}, the DP control law is calculated by setting the SoC as the state variable, i.e., $x =$SoC, and ignoring the transient state of the engine speed in power-split mode, i.e., $\dot{\omega}_{\mathrm{e}} = 0$. Before calculating the DP control law, we must discretize the control variables $\tau_{\mathrm{e}}(k) \in \Omega_{\tau_{\mathrm{e}}}$ and $\omega_{\mathrm{e}}(k) \in \Omega_{\omega_{\mathrm{e}}}$. In this case, the problem becomes a combination optimization problem. Moreover, using the deduced models (27a), (28a) and (29a) and the presented method for calculating the desired driving torque, the speeds and torques of the motor and generator can be calculated at each step k along with $T_{\mathrm{drive}}^{p}(k)$ $(p = \mathrm{I}, \mathrm{II}, \mathrm{III})$, which is calculated from (30)$\sim$(32) in each mode. Furthermore, the state variable SoC is discretized to store the partial-optimal solution at each discrete point. Finally, the optimal control problem is formulated as follows:

$$\begin{cases} \min\limits_{u(k)} \sum\limits_{k=0}^{N-1} [m_{\mathrm{f}}(k) + \Gamma_{\mathrm{e}} m_{\mathrm{e}}(k)]\Delta t \\ \text{s.t. } v(k) = v_{\mathrm{d}}(k), \\ \quad \mathrm{SoC}(k+1) = f(\mathrm{SoC}(k), u(k), T_{\mathrm{drive}}^{i}(k)), \quad (i = \mathrm{I}, \mathrm{II}, \mathrm{III}), \\ \quad \mid \mathrm{SoC}(0) - \mathrm{SoC}(N) \mid \leqslant 0.005, \\ \quad (u_{\mathrm{c}1}(k), u_{\mathrm{c}2}(k)) \in \{(0,0), (1,1), (0,1)\}, \\ \quad \tau_{\mathrm{emin}}(\omega_{\mathrm{e}}(k)) \leqslant \tau_{\mathrm{e}}(k) \leqslant \tau_{\mathrm{emax}}(\omega_{\mathrm{e}}(k)), \\ \quad \tau_{\mathrm{mmin}}(\omega_{\mathrm{m}}(k)) \leqslant \tau_{\mathrm{m}}(k) \leqslant \tau_{\mathrm{mmax}}(\omega_{\mathrm{m}}(k)), \\ \quad \tau_{\mathrm{gmin}}(\omega_{\mathrm{g}}(k)) \leqslant \tau_{\mathrm{g}}(k) \leqslant \tau_{\mathrm{gmax}}(\omega_{\mathrm{g}}(k)), \end{cases} \tag{38}$$

where $\tau_{p\mathrm{mim}}$ and $\tau_{p\mathrm{max}}$ $(p = \mathrm{e}, \mathrm{m}$ or $\mathrm{g})$ denote the corresponding speed-dependent torque limitations of the engine, motor and generator, respectively.

Furthermore, the stored partial-optimal solution of Problem (38) is obtained by the following recursive function of DP, which derives from the Bellman optimization principle.

$$V_{x_k}^{*} = \min V_{x_k}^{\mathrm{set}}, \tag{39a}$$

Table 2 Setting conditions in the DP optimization

Case number	Δx	$\Delta\tau_{\mathrm{e}}$ (Nm)	$\Delta\omega_{\mathrm{e}}$ (rpm)
Case 1	0.1	1	50
Case 2	0.01	5	50
Case 3	0.01	1	100
Case 4	0.01	1	50

Table 3 Simulation results under each condition with respect to $v_{\mathrm{d}}^{\mathrm{I}}$

Case number	Calculation time (min)	Total cost (g)	Distance per liter (km/L)
Case 1	8.2	124.9	64.50
Case 2	17.7	122.7	65.69
Case 3	42.0	122.8	65.64
Case 4	95.3	122.7	65.69

Table 4 Simulation results under each condition with respect to $v_{\mathrm{d}}^{\mathrm{II}}$

Case number	Calculation time (min)	Total cost (g)	Distance per liter (km/L)
Case 1	10.1	147.0	59.53
Case 2	22.4	145.4	60.19
Case 3	47.4	145.3	60.25
Case 4	70.0	145.2	60.25

$$u_{x_k}^* = \arg\min V_{x_k}^{\mathrm{set}}, \tag{39b}$$

$$\text{where } V_{x_k}^{\mathrm{set}} = \{V_{x_k} | V_{x_k} = g_{u_k} + V_{x_{k+1}}^*,\ g_{u_k} \in G_{x_k}\}, \tag{39c}$$

$$G_{x_k} = \{g_{u_k} | g_{u_k} = (m_{\mathrm{f}}(k) + \Gamma_{\mathrm{e}} m_{\mathrm{e}}(k))\Delta t,\ u_k \in U_{x_k}\}. \tag{39d}$$

In the above equations (39), $V_{x_k}^*$ is the minimum total cost from $x(k)$ to $x(N)$, $u_{x_k}^*$ is the partial-optimal solution at $x(k)$, G_{x_k} is the set of partial costs from $x(k)$ to $x(k+1)$, and U_{x_k} is the set of Cartesian products of $u(k)$ satisfying the constraint conditions of the control problem (38). The proposed control problem was solved along two driving routes, $v_{\mathrm{d}}^{\mathrm{I}}$ and $v_{\mathrm{d}}^{\mathrm{II}}$. The state was discretized as $x \in [0.01 : \Delta x : 0.99]$, $\Omega_{\tau_{\mathrm{e}}} = [0 : \Delta\tau_{\mathrm{e}} : 150]$ (Nm), and $\Omega_{\omega_{\mathrm{e}}} = [0 : \Delta\omega_{\mathrm{e}} : 5500]$ (rpm). The control step was $\Delta t = 1$ (s). Additionally, the fuel-electricity equivalent weighting factor Γ_{e} critically affects the solution: the larger the value, the lower the amount of consumed electricity. This control problem was designed only to illustrate the application of the deduced HEV model. Therefore, it assumes a fixed cost function with a constant Γ_{e} ($= 0.0129$). The influence of Γ_{e} on the control design will be investigated in further work. The problem is solved in four cases with different discrete widths of the variables Δx, $\Delta\tau_{\mathrm{e}}$ and $\Delta\omega_{\mathrm{e}}$. The setting conditions are listed in Table 2.

To validate the control law, the developed mechanical models (27)$\sim$(29) were incorporated into an HEV simulator. Assuming the parameters of a prototype industrial HEV, the constructed simulator behaved similarly to the industrial experimental result. Next, the DP control laws in the proposed four cases were successively applied to the simulator. The performances of the solutions in the four cases in $v_{\mathrm{d}}^{\mathrm{I}}$ and $v_{\mathrm{d}}^{\mathrm{II}}$ are presented in Tables 3 and 4, respectively. In both driving routes, the approximate optimal solutions were quickly calculated, and reducing the discrete widths of both the state and control variables reduced the total cost. On the other hand, the economy performances of the fuel consumption were similar in Cases 1 and 4, meaning that when the discrete width of the state SoC is less than 0.1, the solution minimally affects the optimal control result. Furthermore, as only the steady-state engine rotation speed was considered, the energy management solution was highly efficient (as evidenced by the distances traveled per liter of fuel in Tables 3 and 4). Figures 4 and 5 show the sequences of the clutch operations in the four cases of driving routes $v_{\mathrm{d}}^{\mathrm{I}}$ and $v_{\mathrm{d}}^{\mathrm{II}}$, respectively. The curves show that the powertrain operated in parallel mode at high vehicle speeds and at moments of fast acceleration. The operating modes were almost identical in Cases 2–4. This observation explains the similar fuel economy performances of Cases 2–4 in Tables 3 and 4. Finally, to show the instantaneous operation of each power

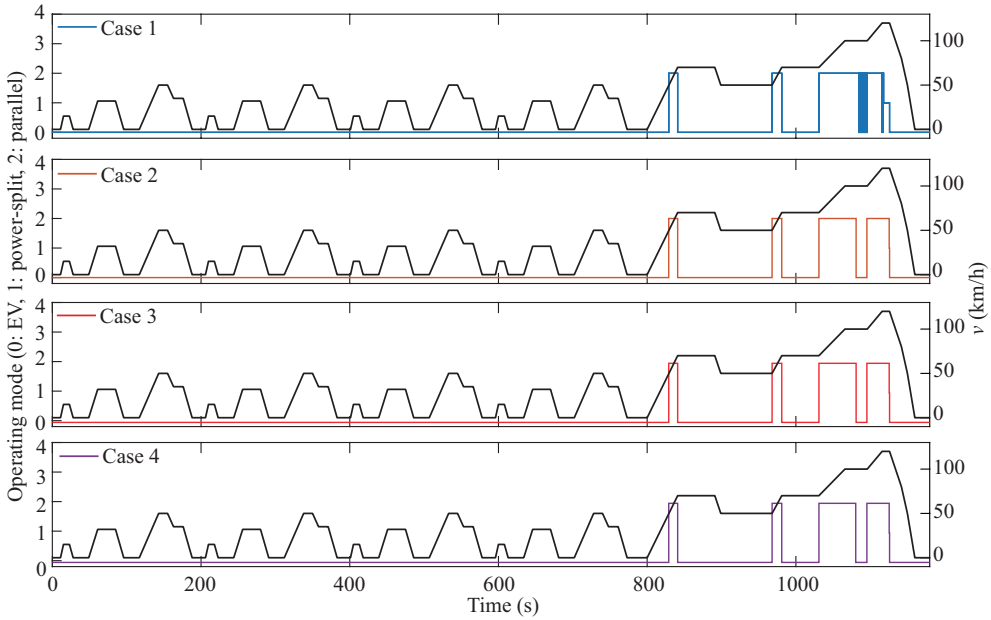

Figure 4 (Color online) Clutch operations of the optimal solutions for different cases in route $v_{\mathrm{d}}^{\mathrm{I}}$.

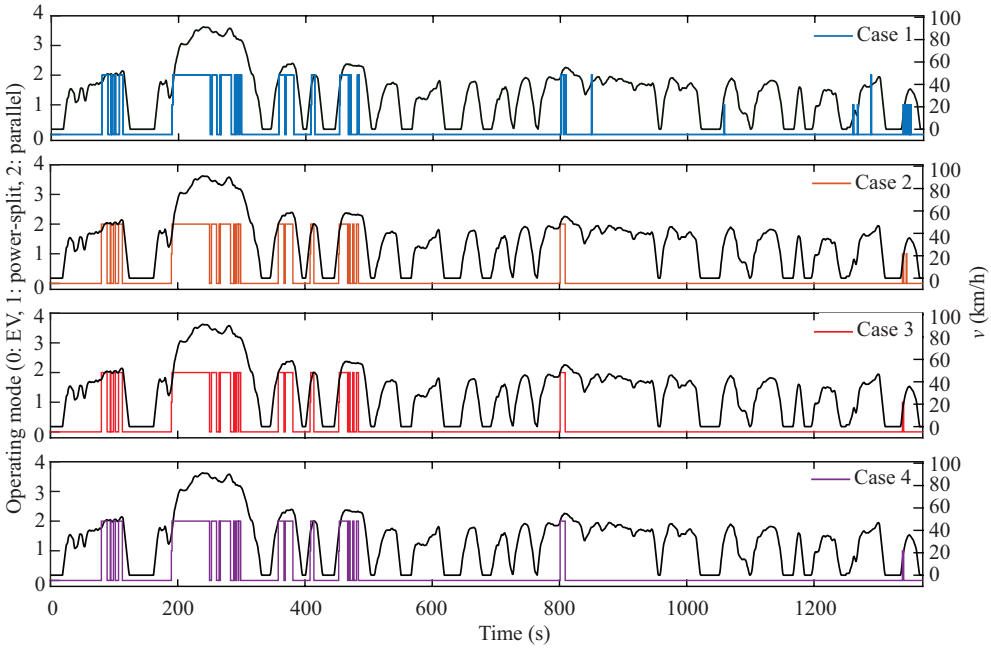

Figure 5 (Color online) Clutch operations of the optimal solutions for different cases in route $v_{\mathrm{d}}^{\mathrm{II}}$.

device, Figures 6 and 7 plot the torque commands and corresponding rotational speeds of the engine, motor, and generator in Case I of driving route $v_{\mathrm{d}}^{\mathrm{I}}$. Figure 8 presents the corresponding SoC curves and instantaneous total costs.

5 Conclusion

This paper presented exact dynamical models for an HEV powertrain with two PG units. The transmission system equips the PG units with two clutches, whose states determine the operating mode (EV, parallel, or power-split) of the mechanical powertrain system. Three dynamical models characterizing the exact behaviors of the powertrain in each operating mode were derived. The EV and parallel modes were

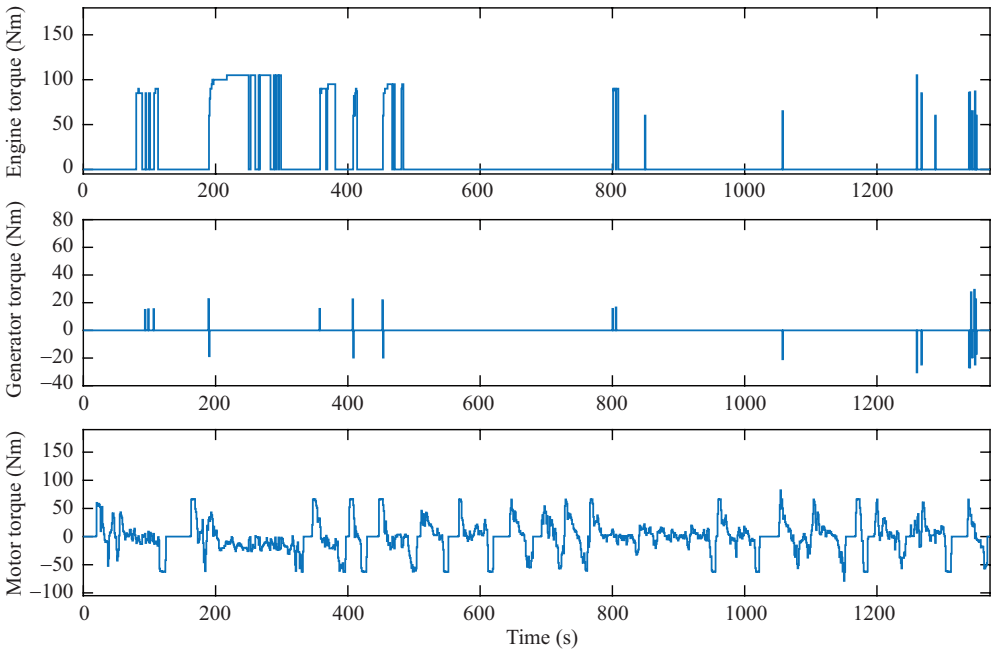

Figure 6 (Color online) Torques of the optimal solutions for different cases in route $v_{\mathrm{d}}^{\mathrm{II}}$.

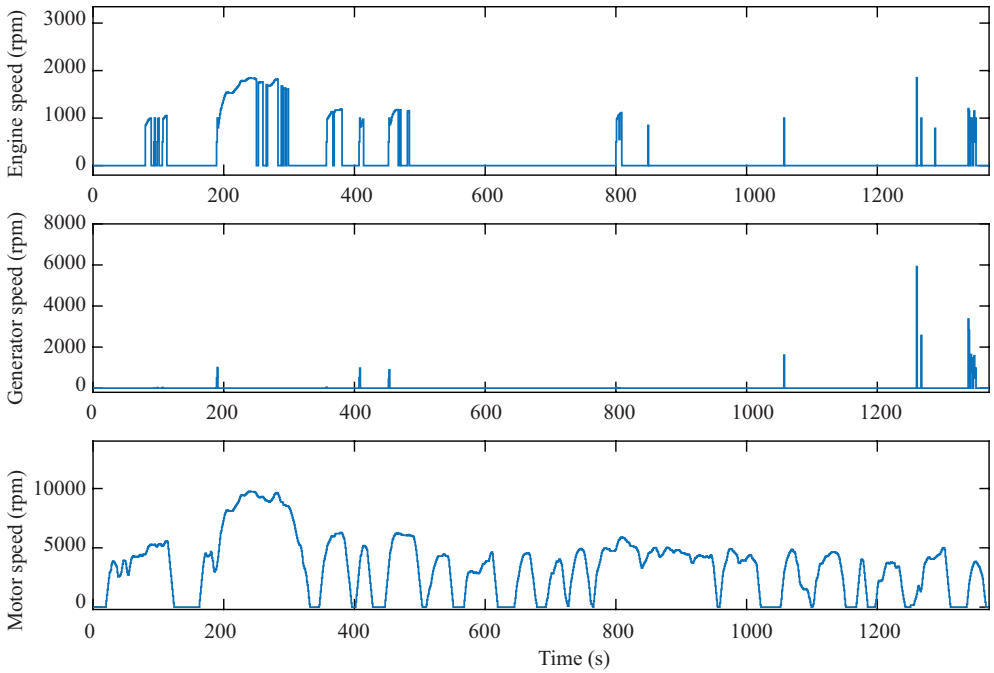

Figure 7 (Color online) Speed outputs for different cases in route $v_{\mathrm{d}}^{\mathrm{II}}$.

described by one-dimensional dynamical models with different inertias, whereas the power-split operating mode was described by a two-dimensional dynamical model involving the vehicle and engine speeds. The proposed models calculate the exact demand-driving torque, which is essential for optimizing the power distribution control of the HEV, particularly during transient operations. To evaluate the proposed dynamical models, the logical variables of the clutch states and engine operating points were taken as the control inputs to a DP-based optimal control problem. Although the DP control law was not formulated for real-time implementation, it demonstrated the significance of the developed models in HEVs with two PGs and two clutches. Ongoing work is focused on real-time energy optimization strategies during

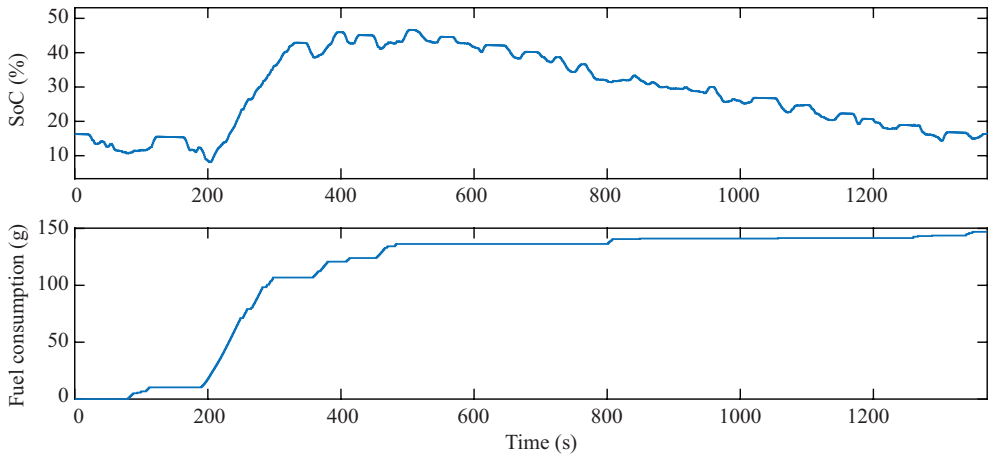

Figure 8 (Color online) SoC outputs and total costs for different cases in route $v_{\mathrm{d}}^{\mathrm{II}}$.

transient operation modes of the vehicle.

References

1 Ehsani M, Gao Y, Gay S, et al. Modern Electric, Hybrid Electric, and Fuel Cell Vehicles, Fundamentals, Theory, and Design. 2nd ed. CRC Press LLC, 2010

2 Zhang X W, Li S E, Peng H, et al. Efficient exhaustive search of power-split hybrid powertrains with multiple planetary gears and clutches. J Dyn Sys Meas Control, 2015, 137: 121006

3 Zhang X W, Peng H, Sun J. A near-optimal power management strategy for rapid component sizing of multimode power split hybrid vehicles. IEEE Trans Contr Syst Technol, 2015, 23: 609–618

4 Wang R, Lukic S M. Dynamic programming technique in hybrid electric vehicle optimization. In: Proceedings of IEEE International Electric Vehicle Conference, 2012. 1–8

5 Kim N, Cha S, Peng H. Optimal control of hybrid electric vehicles based on Pontryagin's minimum principle. IEEE Trans Contr Syst Technol, 2011, 19: 1279–1287

6 Chen Z, Mi C, Xu J, et al. Energy management for a power-split plug-in hybrid electric vehicle based on dynamic programming and neural networks. IEEE Trans Veh Technol, 2014, 63: 1567–1580

7 Tang L, Rizzoni G, Lukas M. Comparison of dynamic programming-based energy management strategies including battery life optimization. In: Proceedings of International Conference on Electrical Systems for Aircraft, Railway, Ship Propulsion and Road Vehicles, 2016

8 Guo L L, Chen H, Gao B Z, et al. Energy management of HEVs based on velocity profile optimization. Sci China Inf Sci, 2019, 62: 089203

9 Borhan H, Vahidi A, Phillips A M, et al. MPC-based energy management of a power-split hybrid electric vehicle. IEEE Trans Contr Syst Technol, 2012, 20: 593–603

10 Zhang J, Shen T. Real-time fuel economy optimization with nonlinear MPC for PHEVs. IEEE Trans Contr Syst Technol, 2016, 24: 2167–2175

11 Guo L, Gao B, Li Y, et al. A fast algorithm for nonlinear model predictive control applied to HEV energy management systems. Sci China Inf Sci, 2017, 60: 092201

12 Moura S J, Fathy H K, Callaway D S, et al. A stochastic optimal control approach for power management in plug-in hybrid electric vehicles. IEEE Trans Contr Syst Technol, 2011, 19: 545–555

13 Di Cairano S, Bernardini D, Bemporad A, et al. Stochastic MPC with learning for driver-predictive vehicle control and its application to HEV energy management. IEEE Trans Contr Syst Technol, 2014, 22: 1018–1031

14 Zhang J, Wu Y. A stochastic logical model-based approximate solution for energy management problem of HEVs. Sci China Inf Sci, 2018, 61: 070207

15 Zhuang W, Zhang X, Li D, et al. Mode shift map design and integrated energy management control of a multi-mode hybrid electric vehicle. Appl Energy, 2017, 204: 476–488